Metallic Si(111)-(7×7)-reconstruction: A surface close to a Mott-Hubbard metal-insulator transition

R. Schillinger,* C. Bromberger, H. J. Jänsch, H. Kleine, O. Kühlert, and C. Weindel
Philipps-Universität, Fachbereich Physik und Zentrum für Materialwissenschaften, D-35032 Marburg, Germany

D. Fick
Philipps-Universität, Fachbereich Physik und Zentrum für Materialwissenschaften, D-35032 Marburg, Germany
and Fritz-Haber-Institut der Max-Planck-Gesellschaft, Faradayweg 4-6, D14195 Berlin, Germany
(Received 7 January 2005; revised manuscript received 5 July 2005; published 14 September 2005)

Li adsorption at extremely low coverages (10^{-3} ML and below) on the metallic Si(111)-(7×7) surface has been studied by β-NMR experiments (measurement of T_1-times). Instead of increasing linearly with the sample temperature, as expected for a metallic system, the relaxation rate $\alpha=1/T_1$ is almost constant in between 50 K and 300 K sample temperature and rises considerably above. Comparison with T_1-times around 900 K (observed with ^{6}Li-NMR) excludes adsorbate diffusion as the cause of the relaxation rate. Thus the almost temperature independent relaxation rate below 300 K points to an extremely localized and thus narrow band (width about 10 meV) which pins the Fermi energy. It is responsible for the metallicity of the (7×7)-reconstruction. Because of the steeply rising relaxation rate beyond 300 K this narrow band is located energetically within a gap (approximately 100–500 meV wide) in between a lower filled and an upper empty (Hubbard) band. Due to its extremely narrow width it can hardly be detected in photo electron experiments. In dynamical mean field theories based on Hubbard Hamiltonians this kind of density of states is typical for correlated electron systems close to a Mott–Hubbard metal-insulator transition.

DOI: 10.1103/PhysRevB.72.115314 PACS number(s): 73.20.At, 68.47.Fg, 76.60.−k, 71.30.+h

I. INTRODUCTION

The band theory of solids is extremely successful in reproducing the ground state properties of solids but breaks down when intrasite Coulomb repulsion of electrons becomes comparable or even larger than the bandwidth.[1,2] With growing Coulomb repulsion the electrons will increasingly localize at the ion cores and electron correlations will be enhanced accordingly. Due to their dangling bond (db) derived states semiconductor surfaces, as e.g., the Si(111) one, constitute a particular class of narrow band systems with band widths well below 1 eV. On the other hand estimates of the effective Coulomb interaction within the dbs of semiconductor surfaces yield typically values of 1–2 eV. Despite an odd number of valence electrons per unit cell semiconductor surfaces may thus become (Mott-Hubbard) insulators.[3,4] The Si(111)-(7×7)-reconstruction seems to be a counterexample; it stays metallic[4,5] since it eliminates a large fraction of its dbs (30 out of 49) by forming the (7×7) structure.[6]

Among the various reconstructions of the Si(111)-surface the (7×7) one is not only by far the oldest example but also the best investigated one.[7–13] (For further, in particular older references, see Ref. 9) Nevertheless there exists up to now no clear-cut picture as to the detailed reasons which causes its metallicity.[3] Over the years theoretical investigations pointed here and there to electron-electron correlation effects.[10,11,14,15] This is supported by the fact that for other reconstructions of the Si(111)-surface, as the Si(111)-(3×1):Li, Si(111)-(1×1):H, SiC(111)-(3×3), etc., correlation effects seem to modify substantially the single particle (electron) picture as well.[4,15–18]

The geometric and energetic properties of the (7×7)-reconstruction are well described within the Dimer-Adatom-Stackingfault (DAS) model.[6,19–22] It leaves 19 dbs of the original 49 ones, one of the corner hole atom, 6 of the rest atoms, and 12 of the adatoms. Experimental and theoretical investigations show that the corner hole and the rest atom dbs are located energetically 1–2 eV below the Fermi level and are thus occupied by two electrons, leaving only 5 electrons for the 12 adatom dbs.[5,10,11,13,19,20,22,23] In an electronic band picture it must be this odd number of electrons in the adatom dbs which eventually causes the "metallicity" of the (7×7)-reconstruction. When, however, beyond this picture correlations become sufficiently strong, as it might be possible for the almost dispersionless state S_1 near the Fermi energy,[24–27] the metallic surface might turn into a Mott insulator.[1,28] As theoretical investigations show this is indeed a realistic possibility.[10,29,30]

On the other hand, the (7×7)-reconstruction has many hallmarks of a metallic surface, at least at room temperature. Photo emission data exhibit intensity up to the Fermi energy (Refs. 9 and 27, and references therein). Independent of the kind of doping, the Fermi level is strongly pinned indicating a large density of states near the Fermi level.[31,32] But only in recent photoelectron experiments a parabolic surface band (width about 280 meV) has been found at surface temperatures as low as 16 K.[9] This low temperature causes, however, a non negligible surface photo voltage[25,33,34] hampering an accurate energetic localization of this band.

For the discussion of possible correlation (localization) effects within the (7×7)-reconstructed surface, as e.g., a metal-insulator transition, it is important to realize that already 20 years ago, even prior to the establishment of the DAS-model, the temperature dependence of electron-energy-loss-spectra (EELS) pointed to an uncommon surface band

structure of the (7×7)-reconstruction. A very narrow (localized) half-filled state at E_F (width 1–2 meV) was found in the center of a gap in between bands formed by more delocalized electrons.[7,8] Such a density of states distribution is very much reminiscent to the one appearing in single band Hubbard-models if a suitable ratio of onsite Coulomb interaction to the hopping matrix elements (bandwidth) is chosen. (See, e.g., Fig. 9 in Ref. 35, Fig. 2 in Ref. 2, but also the discussion in Refs. 14, 15, and 36.) But as already indicated above this view may be hampered by the recently found dispersing band on the momentum scale of the (7×7)-Brillouin zone.[9] It seems to eliminate any kind of localized orbital models for the Si(111)-(7×7)-surface in the vicinity of E_F. On the other hand, to detect such a narrow state at E_F by photoelectron spectroscopy this would require experiments at sample temperatures as low as possible which are, however, affected by a large surface photo voltage[3,9,34] which is moreover inhomogenious over the surface.[37]

For a comparison with experiment, the incorporation of electron-electron correlations into theoretical predictions is still an unsolved task in general. In particular, a unit cell as large as the (7×7) one with its 12 adatom derived levels near the Fermi energy cannot be described in detail by the single band Hubbard-model used so far.[3] Up to now it has "only" been possible to add to results obtained within Density-Functional-Theory (DFT) electron-electron correlation terms, as on-site Coulomb interaction, etc.[10,15,29,30] The theoretical results achieved that way lack, however, a quantitative agreement with the recent photoemission data mentioned above, for which, as already mentioned, the Fermi energy is not well determined because of surface photovoltage effects. And indeed the authors of this experiment[9] cannot exclude a gap of up to 70 meV below the real Fermi level. In turn this would mean that the recently found dispersing band reflects rather a pseudo Fermi surface.

In view of this complex situation obviously experiments are required which can answer the question of a finite density of states at E_F at temperatures as low as possible without being affected by surface photo voltage effects. We therefore resumed our β-NMR experiments on extremely dilute ^{8}Li adsorbates on the Si(111)-(7×7) surface.[12,38] The total Li coverage amounted to 10^{-3} monolayer (ML) at most. That is in the average one Li atom per 20 (7×7) unit cells. The main emphasis of the experiment was to investigate the temperature dependence of T_1-times of the Li nuclear spins. They describe the depolarization with time of an originally polarized nuclear spin ensemble due to its interaction with fluctuating electronic spins.[39–41] Since the T_1-times observed turn out to be of electronic origin their inverse, the relaxation rates $\alpha=1/T_1$, depend directly on the LDOS(E_F) squared, the square of the Local Density Of States taken at E_F and at the adsorbate nucleus.

As compared to the previous experiments[12,38] it is now possible to extend the present ones to much higher magnetic fields and to much lower temperatures. Whereas high magnetic fields suppress considerably diffusive contributions to the T_1-times, low temperatures proved to enhance spectroscopic details in the past.[7,9,27] Additionally the statistical errors are reduced considerably. Moreover the surface preparation and handling has improved substantially (for details, see Sec. II). In particular we avoided after the initial preparation of the (7×7)-reconstruction any subsequent cleaning cycles by high temperature flashes. Previously they caused after a few cycles a fogging of the surface and thus probably a roughening of it. We rather chose the tedious way to replace the "old" surface by a new one if the Auger signal for carbon and/or oxygen exceeded a certain value (for details, see Sec. II). In order to accomplish this during a time as short as possible, we always started from a wet chemically hydrogen terminated surface which could quickly be transferred into the UHV by a homemade fast load lock. We believe that this measure as a whole finally allowed for the observation of the almost temperature independent T_1-times below 300 K.

But to get this direct access to the density of states at E_F one has to pay the price of measuring a local quantity at the adsorption site of Li. Therefore, given the fact, that the electronic properties of the (7×7)-reconstruction vary spatially,[5,13] the knowledge of the adsorption site is essential for the interpretation of the data. Naively one would assume that Li adsorbs at the adatom dbs. And indeed, there are strong hints as well theoretically as experimentally, that this is true.[42,43]

Due to the low Li-coverage of 10^{-3} ML or even below, the Li-adsorbates inject at most one electron per 20 (7×7)-unit cells into the surface electron gas provided by the 5 electrons with in the 12 adatom dbs. This is a negligible amount. We therefore expect that the properties of the (7×7)-band structure are not altered considerably. The discussion in Sec. IV will show that this interpretation maintains despite the surprising results found.

II. EXPERIMENTAL TECHNIQUE AND SETUP

The experiments conducted at the Max-Planck-Institute for Nuclear Physics in Heidelberg were performed in a dedicated UHV-apparatus (base pressure 5×10^{-11} mbar). Conventional analytical techniques were used along with the β-NMR.[44] The latter utilizes β-decaying nuclear spin polarized radioactive ^{8}Li atoms as a probe. A homemade fast load lock is connected to the UHV-chamber. It provides rapid transfer of the wet chemically prepared hydrogen terminated Si(111)-(1×1):H samples used. Details of the load lock concept, of the wet chemical treatment and of the transfer to UHV can be found elsewhere.[12,45] The highly ordered wet chemically hydrogenated surface is termed "hydrogen terminated" in accordance with the literature.[45,46] Heating was available by electron bombardment from the rear, cooling by contact to a liquid helium reservoir, instead of a LN_2 one as in previous experiments.[12,18,38] The lowest temperature reached at the Si crystal was 50 K.

The cleanliness of the surface was monitored by AES. For a "clean surface" the ratios of O(*KLL*)/Si(*KLL*) and/or C(*KLL*)/Si(*KLL*) Auger-intensities had to be below 0.02. In contrast to the previous experiments we avoided to clean samples after preparation of the (7×7)-reconstruction by flashing them beyond 1200 K in order to desorb contaminations as oxygen and carbon, since previously, after several cleaning cycles, a white fogging was observed optically.[47] As

LEED data did not show in parallel correlated changes, we guess now, on the experience of our new results, that the fogging is connected to a roughening of the surface on a length scale beyond the transfer length of LEED experiments.

In order to exchange freshly prepared surfaces as quick as possible we started with hydrogen terminated Si(111)-(1×1):H surfaces which were prepared outside the UHV-chamber by a wet chemical procedure.[12,46,48] Thus we deal outside the UHV-chamber with rather inert surfaces, which moreover are improved in their properties during the wet chemical treatment.[12] After the sample was transferred into the UHV it was flashed to about 1200 K in order to remove the adsorbed hydrogen. Afterwards a gentle cooling process (3 K/s) followed to transfer the (1×1)-reconstruction into the (7×7) one. A clear (7×7) LEED pattern was observed only if this procedure started at sufficiently high temperatures from a well developed (1×1)-reconstruction.

An important but unusual instrument is the source providing a polarized ^{8}Li atomic beam of thermal velocity.[44] At the site of the sample it provides a thermal atomic beam of about 10^8 atoms/s, mainly the primary ^{7}Li used for the production of the ^{8}Li in the ^{2}H(^{7}Li,^{8}Li)^{1}H nuclear reaction. The beam contains a small amount of about 10^4 atoms/s of the nuclear spin polarized radioactive isotope ^{8}Li (polarization 0.8–0.9). ^{8}Li is a β-decaying nucleus with a half life of $T_{1/2}=0.84$ s. Spin polarization of the adsorbate ^{8}Li itself can therefore be detected via the directional asymmetry of the β-decay. The asymmetry ε of the β-electron intensity with respect to the magnetic field is measured by scintillator telescopes at 0° and 180°: ε is proportional to the nuclear polarization of the adsorbed ^{8}Li ensemble. Systematic errors in the determination of ε are eliminated by performing the experiment with the reversed ^{8}Li beam polarization as well. During the β-electron detection period the ^{7}Li ion beam, as the main source of background signals, is switched off.

^{8}Li possesses a nuclear spin $I=2$. Therefore the decay of nuclear polarization with time (relaxation) in general can be expressed as the sum of four exponentials.[49] It is not always possible to disentangle them with high enough precision. However, the slowest relaxation rate could always be determined accurately. Therefore we concentrate in this paper on $\alpha_{\mathrm{slow}} \hat{=} \alpha = 1/T_1$ only in describing $\varepsilon(t)$,

$$\varepsilon(t) = \varepsilon_0 \mathrm{e}^{-\alpha t} = \varepsilon_0 \mathrm{e}^{-t/T_1}. \quad (1)$$

As examples the measured asymmetries ε versus time are shown for 101 K, 296 K, and 412 K in Fig. 1 together with fits of Eq. (1) to the data (solid lines). It is a well known phenomenon in these experiments that the start asymmetry $\varepsilon_0=\varepsilon(t=0)$ varies with surface temperature.[50]

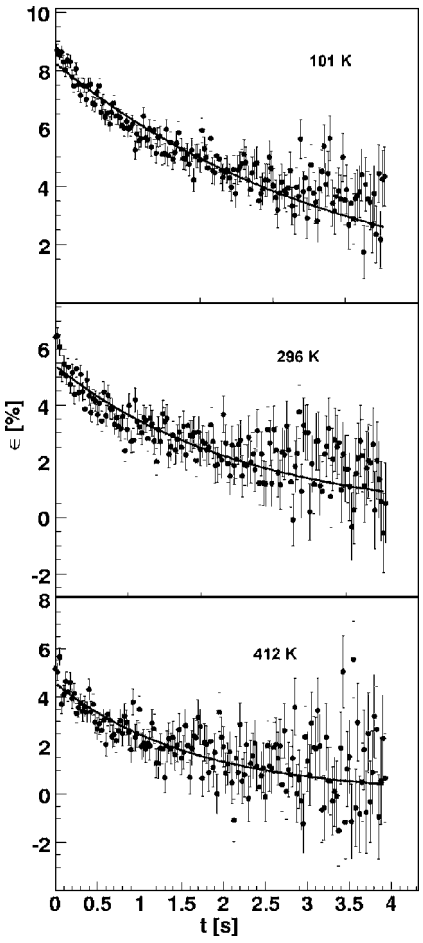

FIG. 1. Observed asymmetry ε versus time for ^{8}Li adsorbed on a Si(111)-(7×7) surface at a magnetic field of 0.8 T and at 101 K, 296 K, and 412 K surface temperature, respectively. The solid line displays a fit of Eq. (1) to the data. The values of α found are plotted in Figs. 2 and 4.

III. EXPERIMENTAL RESULTS AND DISCUSSION

A. Experimental results

In Fig. 2 the observed nuclear spin relaxation rates (inverse T_1-times) obtained at a magnetic field of 0.8 T, are plotted as a function of surface temperature. The open points are from a previous β-NMR experiment[51,52] which results led to the more detailed study here. Both data sets agree well with each other and exhibit a quite unusual temperature dependence. (These data are displayed on an expanded temperature scale in Figs. 4 and 5.) At low temperatures (up to about 300 K) the data are temperature independent. This is in contrast to the results of the previous experiments which started with oxidized Si-samples and used frequent heating cycles up to 1200 K to clean the surface from oxygen and carbon contaminations. There, within quite large error bars, a linear increase of the relaxation rates was observed.[12,38] As will be argued within the discussion of our model describing the new data at the end of Sec. III C, this change in temperature dependence is probably correlated with our new surface preparation technique.

Beyond 500 K the relaxation rates rise, however, considerably up to 900 K where they join smoothly into the values (crosses) found in another NMR-experiment using ^{6}Li as an adsorbate.[52,54] The nuclei ^{6}Li and ^{8}Li by chance possess almost identical nuclear gyromagnetic ratios γ_n. This allows us to compare relaxation rates directly, if they are of electronic origin [for details, see Eq. (6)]. For completeness it should

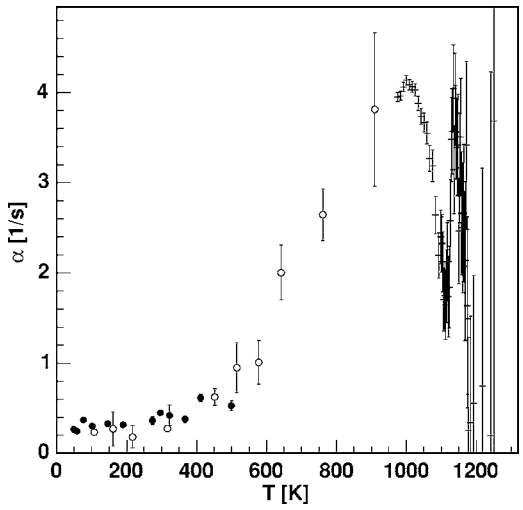

FIG. 2. Temperature dependence of the relaxation rates of Li adsorbed on a Si(111)-(7×7) surface: the open and closed circles are obtained in β-NMR experiments on ^{6}Li as described above at a magnetic field of 0.8 T. The crosses are obtained with ^{6}Li by an other technique (Ref. 53) at 32 mT.

also be noted that these data (crosses) were taken at a much lower magnetic field of 32 mT.

B. Relaxation mechanisms

An ensemble of nuclear spins in a static magnetic field B is driven to its equilibrium m-state distribution through the coupling of its magnetic and/or electric nuclear moments to electromagnetic fields fluctuating in time. The interaction of nuclear moments with static electromagnetic fields leads to an energetic splitting of the nuclear m-states. In most cases and also here, the magnetic Zeeman-interaction dominates and thus the splitting of the m-states is close to the Larmor frequency $\omega_L = \gamma_n B$. Contrary to static fields, transitions between the m-states occur when the nuclear and/or electric moments are coupled to electromagnetic fields fluctuating in time on the order of $1/\omega_L$. Given a sufficiently long time this leads to an equilibrium population of the m-states and thus to an essentially "unpolarized" ensemble as compared to the one we started with in the experiment (polarization around one). The time T_1 which is needed to reach equilibrium depends on the magnitude of the Fourier components of the fluctuating fields at ω_L [see Eqs. (2)–(4)]. From this general picture it becomes clear that T_1-times bear information on any type of dynamical processes which couple strongly enough to the nuclear moments.

Since the fluctuating interactions in general are weak as compared to the static ones (mainly with the external magnetic field), the transition probabilities between the nuclear m-states can be treated in first order perturbation theory. A brief sketch of the theoretical treatment is given in Appendix A of Ref. 49. More details can be found in several monographs[39–41] and in other publications.[12,53,55,56] The latter are chosen such as to deal with surface science problems only.

In what follows we will adopt a phenomenological treatment of the relaxation process and use it for "orders of magnitude" arguments only in order to identify the relaxation mechanism in the present experiments. To describe the frequency spectrum of a fluctuating interaction the time autocorrelation function $G(t)$ and its Fourier transform $j(\omega)$, the spectral density, is used.[39,41,49] According to the BPP model,[57] named after the initials of its authors, the autocorrelation function may be parametrized as

$$G(t) = G(0)e^{-t/\tau_c}. \tag{2}$$

Here $G(0) = \overline{|\mathcal{H}_1(t)|^2}$ denotes the square of the fluctuating interaction, time averaged, and τ_c a proper correlation time, typical for the relaxation process encountered. [For a dominating Zeeman-interaction $G(0)$ does not depend on the m-quantum numbers.] With $G(0)$ from Eq. (2) the Fourier spectrum at the Larmor frequency ω_L is then given by

$$G(0)j(\omega_L) = \frac{1}{\pi}\overline{|\mathcal{H}_1(t)|^2}\frac{2\tau_c}{1+(\omega_L\tau_c)^2}. \tag{3}$$

Relaxation rates are related to $j(\omega_L)$ within a factor of unity by

$$\alpha = \frac{1}{T_1} \simeq \frac{\overline{|\mathcal{H}_1(t)|^2}}{\hbar^2} j(\omega_L)\mathrm{PSF} \tag{4}$$

The phase space factor PSF eventually takes into account that due to Fermi statistics electrons cannot scatter into any energetically allowed state. A closer discussion of the essential entities in Eqs. (3) and (4) as a function of sample temperature and magnetic field for the isotopes ^{6}Li and ^{8}Li will enable us to identify the observed relaxation rates of Fig. 2 as of electronic origin.

The ^{8}Li data below 900 K were determined at a magnetic field of 0.8 T and thus $\omega_L = 3.2\times10^7\ \mathrm{s}^{-1}$ [$\gamma_n(^8\mathrm{Li}) = 3.94\times10^7/\mathrm{T\ s}$]. We start with a discussion of the spectral density $j(\omega_L)$. To begin with we point to the fact that for $\omega_L\tau_c \ll 1$ the spectral density becomes magnetic field independent and proportional to the correlation time τ_c [Eq. (3)]. This situation holds in general for fluctuating delocalized electron spins interacting e.g., via Fermi contact interaction with the nuclear spins. The correlation time is then given by the electron fluctuation time τ_e at a nucleus (atom)[12,58] which can be estimated through $\tau_c \approx \tau_e \approx \hbar/\epsilon_F$.[12,28,59] (Here ϵ_F denotes the value of the Fermi energy counted from the bottom of the band.) Even for strong localization with a bandwidth and thus ϵ_F in the meV region, with which we will deal with below, $\tau_e \approx 10^{-12}$ s and thus still $\omega_L\tau_c \ll 1$.

If the dynamic cause of the fluctuating interaction is diffusion, then the correlation time τ_c is given by the proper hopping time τ_{diff},

$$\tau_c \simeq \tau_{\mathrm{diff}} = \tau_0 e^{E_{\mathrm{diff}}/kT}. \tag{5}$$

Thus the relaxation rates α will be thermally activated [Eqs. (3)–(5)], which indeed was observed experimentally on surfaces too.[49,53] In general, the relaxation rate then displays a resonance like behavior in temperature with a maximum at a temperature for which $\omega_L\tau_c = 1$. The temperature at which the "resonance" of the relaxation rate α occurs depends on the other hand through $\omega_L(B)\tau_c = 1$ only weakly (logarithmically) on the external magnetic field [Eqs. (3)–(5)]. For order of

magnitude effects this will be neglected below.

We first focus on the interaction that causes the rise of the relaxation rates beyond 300 K. At a first glance one would guess that according to the discussion above this rise is caused by thermally activated diffusion, e.g., similar to the one observed for Li adsorption on Ru(001).[49] For a diffusion maximum ($\omega_L\tau_c=1$) to occur at about 1000 K, one requires a diffusion energy of about 1 eV using a "typical" prefactor of $\tau_0=10^{-13}$ s.[60,61] Considering the high diffusion energies found for Li adsorption on Si surfaces at higher temperatures[53,62] this does not sound unreasonable. But a fit to the data using Eqs. (3)–(5) gives a very steep increase of α with temperature. (Not shown here, but compare to the upper part of Fig. 6 in Ref. 49.)

The real proof that the ^{8}Li-relaxation rates beyond 400 K cannot be of diffusive origin comes, however, from the fact, that the temperature dependence of α found for ^{8}Li smoothly joins around 900 K within the error bars the ones for ^{6}Li determined with an other method.[53] [Fig. 2; the temperature dependence beyond 1000 K is due to the continuous $(7\times7)\leftrightarrow(1\times1)$ phase transition, which will be discussed in a forthcoming paper.] The isotopes ^{6}Li and ^{8}Li have almost the same gyromagnetic ratio [$\gamma(^6\mathrm{Li})/\gamma(^8\mathrm{Li})=0.994$] but quite different quadrupole moments[63–65] [$Q(^6\mathrm{Li})=-0.08$ fm^2, $Q(^8\mathrm{Li})=+3.27$ fm^2]. The moments enter the averaged fluctuating interaction Hamiltonian $\overline{|\mathcal{H}_1(t)|^2}$ squared.[39,41,49] Due to the almost identical gyromagnetic ratios one therefore expects almost identical relaxation rates for ^{6}Li and ^{8}Li if they are caused by Fermi contact interaction of fluctuating electronic spins with the nuclear magnetic moments (electronic relaxation) [see Eq. (6) below]. This indeed is observed experimentally around the 900 K sample temperature (Fig. 2).

However, the relaxation could be caused by an interaction of the electric nuclear quadrupole moments with electric field gradients as well, generated by the nonisotropic electronic environment of Li adsorbed at an adatom db. Their fluctuations are often caused by diffusion. Then we expect that the ratio of the observed relaxation rates α is proportional to the ratio of the squares of the nuclear quadrupole moments,[49] $Q^2(^8\mathrm{Li})/Q^2(^7\mathrm{Li})\simeq1670$. Since ^{6}Li and ^{8}Li have different nuclear spins $I=1$ and 2, respectively, this factor reduces to $\alpha(^8\mathrm{Li})/\alpha(^7\mathrm{Li})=417$ at most (see Appendix). This is certainly not observed experimentally (Fig. 2). We therefore conclude, that the relaxation rates observed for low coverage ^{8}Li adsorption on the (7×7)-reconstruction must be of electronic origin over the whole temperature range investigated.

For electronic relaxation for which delocalized electrons are essential the PSF of Eq. (4) has to be considered in addition. Nuclear spin relaxation is connected to nuclear spin flips (change in m-value by ±1). To preserve angular momentum the electron spin must flip as well (in the opposite way). Since the electrons have to obey Fermi-statistics the probability of an electron making a transition from a state with kinetic energy E to a state of energy E' must be weighted by $f(E)(1-f(E'))$ [$f(E)$: Fermi distribution]. This is the probability for the initial state to be occupied and the final state to be empty, simultaneously. However, for such a correlated spin flip the change in kinetic energy is so small (at $B=1$ T about 0.1 meV) that the assumption $E=E'$ is legitimate yielding PSF$=f(E)(1-f(E))$. Taking this into account in Eqs. (3) and (4) and assuming a temperature independent fluctuating interaction $\mathcal{H}_1$, as e.g. the Fermi contact interaction between electronic and nuclear spins, yields for real metals relaxation rates linear in sample temperature T, since for a large enough bandwidth of the order of eV the expression for the PSF may safely be replaced by $f(E)(1-f(E))\simeq kT\delta(E-E_F)$. And, indeed, nuclear spin relaxation rates $\alpha=1/T_1$ linear in the sample temperature T are typical for metallic systems (bulk or surfaces).[39,41,49,66,67] This linear temperature dependence is, however, not observed in the present experiment (Fig. 2) despite the (7×7)-reconstruction of the Si(111)-surface is considered to be "metallic."

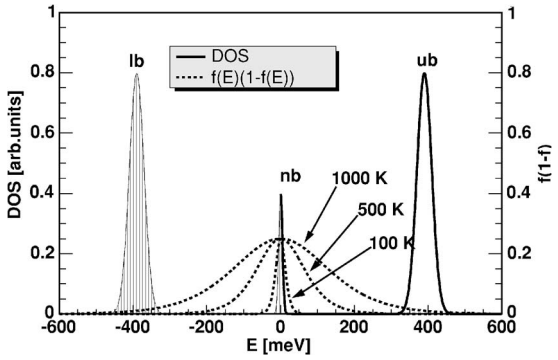

FIG. 3. The model density of states (DOS, solid lines, left scale) and $f(E)(1-f(E))$ [dashed lines, right scale; $f(E)$: Fermi distribution] is displayed as a function of energy ($E_F=E=0$). The parameters were chosen in such a way that a significant picture of the model was obtained. They do not coincide with those found in the fit to the data (Table I).

C. A schematic model

As mentioned within the Introduction, already at the beginning of the 1980s electron-energy-loss spectroscopy (EELS) experiments on the Si(111)-(7×7) surface in between 15 K and 300 K sample temperature yielded among others a highly localized half occupied state (width about 1 meV) which resides within a surface state gap about 100 meV wide.[7,8] It pins the Fermi level position. At about the same time the study of many body effects in the Si(111) surface states with a Hubbard-Hamiltonian showed that such a narrow (localized) surface state may exist, if for electrons in the dangling bonds onsite Coulomb repulsion and hopping matrix elements are properly chosen.[14,36] Those theoretical approaches produce under a wide range of modeling conditions a more or less narrow state at the Fermi energy in between broader lower filled and upper empty (Hubbard) bands.[2,15,35]

For further use below Fig. 3 displays a *schematic* DOS energy distribution which renders the essential features of the experimental results.[68] The adatoms form an extremely narrow band at the Fermi energy located in between broader lower and upper bands.

Since, as already mentioned above, there are strong hints, theoretically as well as experimentally, that Li at low coverages preferentially adsorbs at the adatom dangling bonds.[42,43] Such a level density is also very promising to explain our experimental results. A half filled narrow band, which pins the Fermi energy, will lead to a temperature independent relaxation rate, as long as kT is larger than the width of the band itself. The reason is that $f(E)(1-f(E))$ is temperature independent over the narrow band. (See Fig. 3 where $f(E)(1-f(E))$ and DOS(E) are plotted simultaneously.) Furthermore, an additional wide gap with a filled lower and empty upper band will lead with increasing sample temperature to an enhanced excitation of electrons from the lower to the upper band thus enabling further electron fluctuations and thus an increasing relaxation rate with temperature.

To become more specific we start with an expression of the relaxation rate for which the approximation $f(E)(1-f(E)) \simeq kT\delta(E-E_F)$ has *not* been adopted,[41]

$$\alpha = 2\frac{2\pi}{\hbar}\left(\frac{2}{3}\mu_0\gamma_e\gamma_n\hbar^2\right)^2\frac{1}{4}|\Phi_F(0)|^4 \times \int_0^\infty \mathrm{DOS}(E)^2 f(E)(1-f(E))dE. \quad (6)$$

It was derived from first order perturbation theory assuming Fermi contact interaction between the nuclear (γ_n) and electron (γ_e) magnetic moments only. In contrast to our previous publications[12,18,38] DOS(E) denotes now the electron density of states for one spin direction only. $|\Phi_F(0)|^2$ denotes the probability to find at E_F an electron at the nucleus. The factor $1/4$ stems from integration over k-space, which was assumed to be isotropic. (For surfaces the assumption of an isotropic k-space has probably to be improved if a more quantitative comparison is envisaged in the future. For a more general derivation where this assumption was not made, see Ref. 55.) Replacing in Eq. (6) $f(E)(1-f(E))$ by $kT\delta(E-E_F)$ would yield the well known expression for relaxation on a metal surface.[39–41,49,66]

In order to proceed further we now have to specify analytically the density of states sketched in Fig. 3. To reduce the number of parameters we use either a Gaussian form

$$\mathrm{DOS}_i(E) = \frac{D_i}{\sqrt{2\pi}\sigma_i}e^{-[(E_i-E)^2/2\sigma_i^2]} \quad (7)$$

for the three parts, with $i=l,n,u$ for the lower, narrow, and upper band respectively, or Lorentzian ones

$$\mathrm{DOS}_i(E) = \frac{D_i\sigma_i}{2\pi}\frac{1}{(E_i-E)^2+\sigma_i^2/4}. \quad (8)$$

(For the upper and lower band such density distributions are certainly not the best assumption. But, since for the temperature regime investigated only the lower falling and the upper rising edge counts, this choice is tolerable.) Since the narrow band pins the Fermi energy we chose $E_n=E_F=0$. In order to reduce the number of parameters to be fitted further, we assume symmetric upper and lower bands with respect to the Fermi energy ($E_l=-E_0/2$, $E_u=E_0/2$, $\sigma_l=\sigma_u=\sigma$). As we use normalized functions $D_l=D_u=D$ holds as well. The density of states DOS(E) entering Eq. (6) is now a sum of these three contributions,

$$\mathrm{DOS}(E) = \mathrm{DOS}_l(E) + \mathrm{DOS}_n(E) + \mathrm{DOS}_u(E). \quad (9)$$

With these assumptions still five parameters have to be fitted to the data. The results of such a fit with parameters listed in Table I are plotted as solid lines in Fig. 4. They are indistinguishable for both functions used (Gaussian and Lorentzian).

TABLE I. List of parameters of the model fitted to the data of Fig. 4 which yields the indistinguishable solid lines.

	Gaussian	Lorentzian	
E_0	(577±143)	(445±59)	meV
σ_n	(5.1±2.3)	(6.4±5.0)	meV
σ	(104±32)	(77±25)	meV
$\lvert\Phi_F(0)\rvert^2 D_n$	(4.8±1.5)	(4.6±2.1)	10^{-3} Å^{-3}
$\lvert\Phi_F(0)\rvert^2 D$	(0.17±0.09)	(0.10±0.03)	Å^{-3}
E_{gap}	(332±223)	(368±84)	meV
σ_n(FWHM)	(12.0±5.4)	(6.4±5.0)	meV
σ(FWHM)	(245±80)	(77±25)	meV

Comparing the fit parameters for the Gaussian and Lorentzian density of states distributions we find a fair agreement within the error bars. For the increase of the relaxation rate above 300 K only the rising and falling edge of the upper and lower bands, respectively, matter. Thus E_0 itself, the energetic distance of the centers of the upper and lower rather broad bands is not a meaningful quantity to characterize the gap inbetween them. It is more meaningful to count the gap energy E_{gap} from their FWHM (full width at half maximum) energies respectively, that is,

$$E_{\mathrm{gap}} = E_0 - \tfrac{1}{2}\sigma_l(\mathrm{FWHM}) - \tfrac{1}{2}\sigma_u(\mathrm{FWHM}) = E_0 - \sigma(\mathrm{FWHM}). \quad (10)$$

Moreover to judge the width of the narrow band, its width σ_n(FWHM) seems to be the appropriate quantity to compare results for the Gaussian and Lorentzian distributions. All this latter quantities are listed in the lower part of Table I as well.

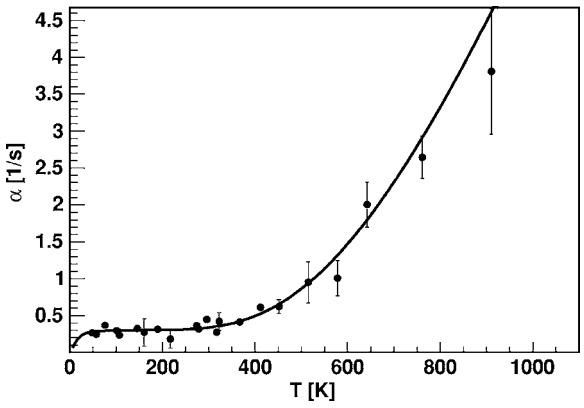

FIG. 4. The ^{8}Li-β-NMR data of Fig. 2 together with the fit to the schematic model [Eqs. (6)–(9)] described in the text.

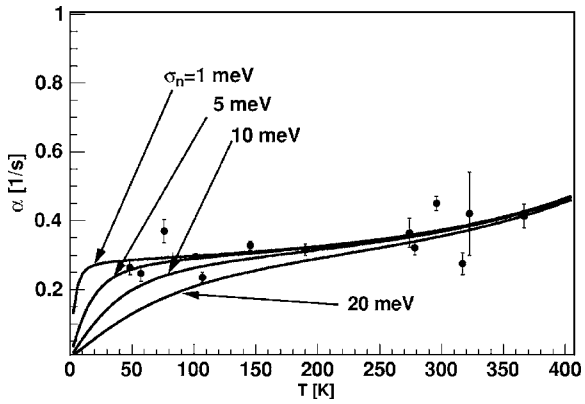

FIG. 5. Results of fits to the data of Fig. 2 for fixed values of the width of the narrow band σ_n in between 1 meV and 20 meV. To display the low temperature part in more detail the results are shown up to 400 K only. (Only Gaussian distributions shown here.)

In order to discuss the result of the fit and in particular the sensitivity of the parameters to the experimental data we start with the remark that as long as $\sigma_n \ll 2kT$ [and as long as the wings of $f(E)(1-f(E))$ do not overlap significantly with DOS_l and DOS_u] we can replace $f(E)(1-f(E))$ in Eq. (6) by 1/4. [The product $f(E)(1-f(E))$ has a "half-width" of $2kT$ and a maximum of 1/4.] Then the relaxation rate becomes almost temperature independent and is proportional to $|\Phi_F(0)|^2 D_n$. Thus the experimental results up to about 300 K directly determine this quantity. {The slight increase of the fit with temperature below 300 K is a consequence that DOS^2 enters the expression of the relaxation rate α [Eq. (6)]. Due to the wings of the distributions "mixed" terms from the u-, n-, and l-bands appear.} The width σ_n itself is determined by the temperature range where $\sigma_n \ll 2kT$ breaks down. To demonstrate the sensitivity of σ_n to the data, Fig. 5 shows the low temperature part of the data together with results for various values of σ_n, but now for the Gaussian DOS distributions only. It is obvious that the value of σ_n extracted from the fit is essentially an upper limit of σ_n. In order to improve this situation data below 50 K are required, a temperature range which unfortunately could not be reached yet with our experimental setup.

At temperatures at which the wings of $f(E)(1-f(E))$ start to overlap considerably with the lower and upper bands, electrons are promoted from the lower to the upper band and contribute to the relaxation rate, which then starts to rise. This determines mainly E_0. (Electrons in a completely filled band do not contribute to the relaxation process since they are not able to flip their spin.) The very increase of α then depends on the shape of the falling and rising edge of the lower and upper band, respectively. This determines their width σ and their strength $|\Phi_F(0)|^2 D$ not in a very transparent way and therefore with rather large error bars. A much more precise determination of the form of the upper and lower band would in principle emerge from data taken at temperatures still higher than 900 K. But as Fig. 2 shows, the $(7\times7)\leftrightarrow(1\times1)$ phase transition starts to influence the relaxation rates already there.

The extremely small width of the state at E_F may also be the reason for the previously observed linear increase of the relaxation rates with temperature.[12,38] This is observable only if the "width" of the electronic density of states considerably exceeds $2kT$, the "width" of $f(E)(1-f(E))$. The previous data were taken from 100 K to 500 K with rather large error bars. As already mentioned in Sec. II, in these experiments probably a roughening of the surface occurred due to the frequent heating cycles applied. Then empty and filled defect states may be present within the band gap, causing a blurred density of states around E_F. If so, the relaxation rate rises with temperature. With large enough error bars (as in the previous experiments) this may look like a linear dependence as expected for real metallic systems.

IV. CONCLUSIONS

The results of the preceding subsection clearly show that the model density of states of Fig. 3 is able to describe the data for both Gaussian and Lorentzian forms. Moreover, it is possible to retrace the values of the parameters found within the fit to certain sections of the observed temperature dependence of the relaxation rates in Fig. 4. However, since the problem is as usual not invertible, i.e., the DOS(E) cannot be inferred directly from the observed temperature dependence of α, in what follows we will judge at least in some detail the consistency of the results found here when compared to others. Before doing so we would like to point out that adsorbed Li is a very local probe, sensing the DOS at its nucleus. Theoretical and experimental investigations point towards an adatom db as adsorption site.[42,43] Since Li is adsorbed here at extremely low coverages of 10^{-3} ML and below, the adsorbed Li will add in average only 1/20th electron to the 5 electrons per (7×7) unit cell within the 12 adatom dbs. Thus we expect that it will not change the overall electronic properties, as the energy dependence of the DOS. However, its local value $[\mathrm{DOS}(E)|\Phi_F(0)|^2]$ may be affected. That is why without detailed calculations the magnitude of the observed α can only be compared in an order of magnitude approach to DOS-calculations for the Si(111)-(7×7) surface.

Most surprising was the temperature independent relaxation rate below 300 K (Figs. 2, 4, and 5). For adsorption on doped semiconductor surfaces it is possible to produce at least theoretically temperature independent relaxation rates in the saturation regime.[18] To our knowledge this has never been observed experimentally on surfaces yet. But it is well known that the saturation regime can only be reached with a changing Fermi level position.[59,69,70] But this is not possible here as the Fermi level is pinned at the (7×7)-reconstructed Si(111)-surface.[31,32] Therefore, as found with the schematic model in the previous subsection, the cause of the Fermi level pinning by the narrow band must also be the reason for the temperature independent relaxation rate.

The width of the narrow band of around 10 meV or below indicates a spatially localized state. It can only arise if strong electron correlations are present, as proposed for the Si(111)-surface in a Hubbard model as early as 1982.[14,36] In between a lower filled and an upper empty Hubbard band a narrow half filled band at E_F was found there. We are therefore tempted to identify the lower and upper band in the present analysis with such Hubbard bands. Our interpretation is sup-

ported by the analysis of EELS-data which found a half-filled band approximately 1–2 meV wide within a roughly 100 meV wide gap.[7] Moreover, using a scanning tunneling microscope (STM) energy resolved real space images of filled and empty states of the Si(111)-(7×7) surface yielded a surface band gap around E_F less than 300 meV wide.[5] (This value was estimated from the lowest positive and negative bias used.) This experiment could not probe states exactly at E_F, but the similarity between images at the lowest positive and negative bias voltages led the authors to the conclusion that they involve tunneling through the same metallic state. We consider these results as a further support of the existence of a gap.

The theoretical analysis with a single band Hubbard-Hamiltonian based on DFT calculations resulted in a potentially more microscopic understanding of the origin of the narrow band at E_F.[10,30] Out of the 19 dangling bonds of the (7×7)-reconstruction (12 adatom, 6 restatom, and 1 corner hole one) those of the restatoms and of the corner hole are doubly occupied. This leaves 5 electrons in the 12 adatom dangling bonds making up the DOS around the Fermi energy. Solutions of the Hubbard many body Hamiltonian including correlation effects (intra- and intersite Coulomb-interaction, hopping matrix elements) show that in the ground state three electrons occupy the so-called ring adatoms and two the three dimer adatoms. The latter leads to a threefold degenerate state responsible for the "metallicity" of the surface. Hopping matrix elements between these two classes of adatoms are found to be small. Thus the electronic structure in the rings (below E_F) is practically decoupled from the degenerate dimer bands. The rings appear isolated within the dimers and behave as a periodic impurity with a donor and acceptor level about 100 meV above and below E_F. If so, the narrow band at E_F might be identified with a "Kondo peak."

Theories using such a Hubbard Hamiltonian lead in general for a proper ratio of hopping matrix elements T to intrasite Coulomb-interaction U to a narrow half filled band in between the lower and upper Hubbard bands.[2,15,35,71,72] [For example, Fig. 9 in Ref. 35 bears an amazing resemblance to the schematic model DOS used to analyze our data (Fig. 3).] From this point of view one is tempted to consider the (7×7)-reconstruction as a system just prior to a Mott-Hubbard metal-insulator transition.

If so, the value of the gap can be estimated from the Coulomb repulsion of an additional electron in an adatom db and the screening response of the crystal to this charge transfer.[3,4] A very rough estimate of the Hubbard U is obtained by setting $U=U^{\mathrm{atom}}/\epsilon_{\mathrm{eff}}\simeq1.2$ eV, where $U^{\mathrm{atom}}=7.64$ eV is the atomic value of an isolated Si sp^3 orbital.[73,74] $\epsilon_{\mathrm{eff}}=(\epsilon_b+1)/2$ is taken as the mean average of the Si-bulk ($\epsilon_b\simeq12$) and the vacuum dielectric constants. The value of $U\simeq1.2$ eV compares favorably with the one ($U=1.1$) found within the single band Hubbard model calculations mentioned already[10,30] but overestimates by far the value found here, if we identify $U=E_{\mathrm{gap}}$ (Table I). This deviation may be due to the rough estimates used. But it may also have a real physical background: As already mentioned above, many adatom dbs-derived levels appear in the projected fundamental gap of the Si(111)-(7×7) surface.[10,15,75] Therefore a single band Hubbard model, as used so far in all discussions, may describe the gross properties but not the detailed consequences of electron correlation in the Si(111)-(7×7) surface.[3]

We finish this subsection in discussing the strength of the narrow band at E_F. The first theoretical treatment, which uses essentially a (1×1) surface, finds about 0.08 electrons per atom ((1×1)-unit cell)[14] which amounts to about 4 electrons per (7×7)-unit cell. The most recent calculations find 2 electrons (in the dimers) per (7×7)-unit cell.[10,30] The analysis of the EELS data yield 1 electron within the 1 meV wide narrow band at E_F.[8] As already mentioned at the beginning of this subsection, these numbers cannot be compared one to one to the ones found experimentally here, since Li is an entirely local probe and it injects one additional electron per adsorbed Li into the adatom dangling bonds. [For a coverage below 10^{-3} this is, however, less than 0.05 electrons per (7×7)-unit cell.]

Fitting the data we found $|\Phi_F(0)|^2D_n=(5\pm2)\times10^{-3}$ Å^{-3} for the amplitude of the narrow band (Table I). Without detailed calculations $|\Phi_F(0)|^2$ is, however, not known. But in a rough interpretation of this number, we may assume that $|\Phi_F(0)|^2$ is smaller than $|\Phi(0)|^2$ the value for the free ^{8}Li-atom which can be calculated from its hyperfine splitting (HFS).[76] This assumption is based on the fact that, due to adsorption, an electric dipole moment is induced on the ^{8}Li-atom which transfers strength from the s-wave part [which determines solely $|\Phi_F(0)|^2$] to the p-wave. From the known HFS $\nu_{\mathrm{hfs}}=382.5$ MHz (Ref. 77) of ^{8}Li we deduce $|\Phi(0)|^2=0.71$ Å^{-3} for the free ^{8}Li-atom and thus $D_n>(0.007\pm0.003)$. Since the distributions used to describe the DOS of the narrow band [Eqs. (7) and (8)] are normalized to one, $D_n>0.004$ indicates a lower limit of the number of electrons per spin direction and per (1×1) unit cell in the narrow band, if the error bars are taken into account additionally. Thus, if the (7×7)-reconstruction is not magnetic, there are at least about 0.4 electrons (both spins) per (7×7) unit cell building up the narrow band at E_F, about an order of magnitude more than the 0.05 electrons injected by the Li adsorbate at a coverage of 10^{-3}. The lower limit of 0.4 electrons in the narrow band is quite in accordance to the results found in the other experimental and theoretical investigations mentioned above.

In summary the experimental data presented here and their analysis point strongly to an understanding of the Si(111)-(7×7)-reconstruction in terms of a surface close to a Mott-Hubbard metal-insulator transition. Typical signatures are the narrow band in between a lower filled and empty upper Hubbard band. Since the narrow band acquires at least half an electron per (7×7) unit cell, it obviously pins the Fermi energy independently of the bulk doping. This is in accordance with photo electron experiments performed so far.[31,32,78]

Because of the extremely narrow width of the band at E_F it will, however, be almost impossible to find it with conventional photoelectron experiments. For such an experiment a surface temperature as low as possible would be required, which in turn would cause a strong surface photo voltage

shift, prohibiting a resolution of 10 meV or below.[9] But a repetition of the HREELS experiment on which the model presented here was based,[7,8] but now with much improved resolution and/or a low temperature STM (STS) experiment[5,13] may be promising to corroborate the interpretation presented here.

ACKNOWLEDGMENTS

This work was supported by the Deutsche Forschungsgemeinschaft (DFG), Bonn (Germany). We acknowledge the invaluable support of the Max-Planck-Institute für Kernphysik, Heidelberg (Germany) at which the experiments were performed. Last but not least we thank Professors F. Bechstedt (Jena), F. Gebhard (Marburg), F. J. Himpsel (Madison), and H. Kroha (Bonn) for fruitful discussions.

APPENDIX

If the relaxation of the nuclear polarization is caused by the interaction of the nuclear electric quadrupole moments with fluctuating electric field gradients (EFGs), the ratio of the relaxation rate $\alpha(^8\mathrm{Li})/\alpha(^6\mathrm{Li})$ for adsorbed ^{8}Li and ^{6}Li depends on the ratio of the quadrupole moments of ^{8}Li and ^{6}Li squared times a factor which depends on details of the EFG-tensor, the values of the nuclear spins, and on the spectral densities. To obtain this factor explicitly we follow without further comments the arguments in Appendix A1 of Ref. 49 including the notation used there.

The ^{8}Li experiments have been performed with ^{8}Li adsorbates ($I=2$) prepared predominately either in the $m=+2$ or $m=-2$ magnetic sublevel of its nuclear spin. Therefore, the polarization of the ^{8}Li adsorbates is a superposition of rank 1 to rank 4 polarization. β-decay asymmetries ϵ are sensitive to rank 1 polarization only, which is just called polarization in the main text. The complexity of what follows arises from the fact that the time dependence of first and third rank polarization are coupled through the interaction of the ^{8}Li electric quadrupole moment with fluctuating EFGs. Since ^{6}Li possesses only $I=1$ and thus rank 2 polarization at most, such a coupling is not present for this nucleus.

The coupling of first and third rank polarization leads to "fast" and "slow" relaxation rate α_- and α_+ respectively [e.g., Eq. (A10) in Ref. 49] from which only the slow component $\alpha_+=\alpha_{\mathrm{slow}}\hat{=}\alpha$ was observed experimentally here [Eqs. (1) and (A13) from Ref. 49]. Inserting, from Ref. 49 Eq. (A7) into Eq. (A11), one yields explicitly for

$$\alpha(^8\mathrm{Li}) = \frac{w(^8\mathrm{Li})}{2}(63 + 80\kappa + \sqrt{3425 + 304\kappa + 1600\kappa^2}). \tag{11}$$

The quantity "w" denotes a kind of a strength factor

$$w = \frac{1}{80}\frac{(eQ)^2}{\hbar^2}|V_{21}|^2 j(\omega_L) \tag{12}$$

and κ a double ratio,

$$\kappa = \frac{\overline{|V_{22}|^2}}{\overline{|V_{21}|^2}}\frac{j(2\omega_L)}{j(\omega_L)}. \tag{13}$$

$\overline{|V_{2q}|^2}(q=1,2)$ are the time averaged absolute squared spherical components of the fluctuating EFG and $j(\omega_L)$ the spectral densities [Eq. (3)] at the frequencies indicated. Since the gyromagnetic ratios for ^{8}Li and ^{6}Li are almost identical, $j(2\omega_L)$ and $j(\omega_L)$ and thus κ does not depend on the isotope used.

Using for ^{6}Li the same formalism as sketched in Ref. 49, for which more details can be found elsewhere,[39,79] one obtains for the nuclear spin relaxation rate of ^{6}Li driven by fluctuating EFGs under the same assumptions as made for ^{8}Li,

$$\alpha(^6\mathrm{Li}) = \frac{w(^6\mathrm{Li})}{2}(120 + 480\kappa). \tag{14}$$

Thus using Eqs. (11)–(14) the ratio of the relaxation rate for ^{8}Li and ^{6}Li is given by

$$\frac{\alpha(^8\mathrm{Li})}{\alpha(^6\mathrm{Li})} = \frac{Q^2(^8\mathrm{Li})}{Q^2(^6\mathrm{Li})}r(\kappa), \tag{15}$$

with

$$r(\kappa) = \frac{63 + 80\kappa + \sqrt{3425 + 304\kappa + 1600\kappa^2}}{120 + 480\kappa}. \tag{16}$$

It now matters that κ is always positive varying in between 0 and $+\infty$. Over this interval $r(\kappa)$ is a positive monotonically falling function from $r(0)=1.01$ to $r(\infty)=0.25$. Thus inserting the quadrupole moments of ^{8}Li and ^{6}Li one obtains as lower limit for the ratios of the relaxation rate at a fixed temperature $\alpha(^8\mathrm{Li})/\alpha(^6\mathrm{Li}) \geqslant 417.5$.

*Email address: richard.schillinger@psi.ch; Current address: Paul Scherrer Institut(PSI), CH-5232 Villigen, Switzerland

[1] N. F. Mott, *Metal-Insulator Transitions*, 2nd ed. (Taylor and Francis, London, 1990).
[2] G. Kotliar and D. Vollhardt, Phys. Today **57**(3), 53 (2004).
[3] F. Bechstedt, *Principles of Surface Physics* (Springer, Berlin, 2003).
[4] F. Bechstedt and J. Furthmüller, J. Phys.: Condens. Matter **16**, S1721 (2004).
[5] R. J. Hamers, R. M. Tromp, and J. E. Demuth, Phys. Rev. Lett. **56**, 1972 (1986).
[6] K. Takayanagi, Y. Tanishiro, S. Takahashi, and M. Takahashi, Surf. Sci. **164**, 367 (1985).
[7] J. E. Demuth, B. N. J. Persson, and A. J. Schell-Sorokin, Phys. Rev. Lett. **51**, 2214 (1983).
[8] B. N. J. Persson and J. E. Demuth, Phys. Rev. B **30**, 5968 (1984).
[9] R. Losio, K. N. Altmann, and F. J. Himpsel, Phys. Rev. B **61**, 10845 (2000).

[10] J. Ortega, F. Flores, and A. L. Yeyati, Phys. Rev. B **58**, 4584 (1998).
[11] F. Flores, A. L. Yeyati, and J. Ortega, Surf. Rev. Lett. **4**, 281 (1997).
[12] H. Winnefeld, M. Czanta, G. Fahsold, H. J. Jänsch, G. Kirchner, W. Mannstadt, J. J. Paggel, R. Platzer, R. Schillinger, R. Veith, C. Weindel, and D. Fick, Phys. Rev. B **65**, 195319 (2002).
[13] R. Wolkow and P. Avouris, Phys. Rev. Lett. **60**, 1049 (1988).
[14] E. Louis, F. Flores, F. Guinea, and C. Tejedor, Solid State Commun. **44**, 1633 (1982).
[15] F. Flores, J. Ortega, and R. Pérez, Surf. Rev. Lett. **6**, 411 (1999).
[16] C. Bromberger, J. N. Crain, K. N. Altmann, J. J. Paggel, F. J. Himpsel, and D. Fick, Phys. Rev. B **68**, 075320 (2003).
[17] X. Blase, X. Zhu, and S. G. Louie, Phys. Rev. B **49**, 4973 (1994).
[18] C. Bromberger, H. J. Jänsch, O. Kühlert, R. Schillinger, and D. Fick, Phys. Rev. B **69**, 245424 (2004).
[19] D. R. Alfonso, C. Noguez, D. A. Drabold, and S. E. Ulloa, Phys. Rev. B **54**, 8028 (1996).
[20] H. Lim, K. Cho, I. Park, J. D. Joannopoulos, and E. Kaxiras, Phys. Rev. B **52**, 17231 (1995).
[21] J. Kim, M.-L. Yeh, F. S. Khan, and J. W. Wilkins, Phys. Rev. B **52**, 14709 (1995).
[22] C. Noguez, A. I. Shkrebtii, and R. D. Sole, Surf. Sci. **331–333**, 1349 (1995).
[23] R. M. Tromp, R. J. Hamers, and J. E. Demuth, Science **234**, 304 (1986).
[24] P. Martensson, W.-X. Ni, G. V. Hansson, J. M. Nicholls, and B. Reihl, Phys. Rev. B **36**, 5974 (1987).
[25] J. E. Demuth, W. J. Thompson, N. J. DiNardo, and R. Imbihl, Phys. Rev. Lett. **56**, 1408 (1986).
[26] F. J. Himpsel, D. E. Eastman, P. Heimann, B. Reihl, C. W. White, and D. M. Zehner, Phys. Rev. B **24**, 1120 (1981).
[27] R. I. G. Uhrberg, T. Kaurila, and Y.-C. Chao, Phys. Rev. B **58**, R1730 (1998).
[28] J. M. Ziman, *Principles of the Theory of Solids* (Cambridge University Press, Cambridge, 1964).
[29] J. Ortega, A. L. Yeyati, and F. Flores, Appl. Surf. Sci. **123/124**, 131 (1998).
[30] J. Ortega, F. Flores, R. Pérez, and A. L. Yeyati, Prog. Surf. Sci. **59**, 233 (1998).
[31] F. J. Himpsel, G. Hollinger, and R. A. Pollak, Phys. Rev. B **28**, 7014 (1983).
[32] F. J. Himpsel and T. Fauster, J. Vac. Sci. Technol. A **2**, 815 (1984).
[33] K. Horn, Appl. Phys. A: Solids Surf. **51**, 289 (1990).
[34] M. Alonso, R. Cimino, and K. Horn, Phys. Rev. Lett. **64**, 1947 (1990).
[35] P. Pou, R. Pérez, F. Flores, A. L. LevyYeyati, A. Martin-Rodero, J. Blanco, F. J. Garcia-Vidal, and J. Ortega, Phys. Rev. B **62**, 4309 (2000).
[36] E. Louis, C. Tejedor, and F. Flores, Solid State Commun. **47**, 939 (1983).
[37] F. J. Himpsel (private communication, 2005).
[38] D. Fick, R. Veith, H. D. Ebinger, H. J. Jänsch, C. Weindel, H. Winnefeld, and J. J. Paggel, Phys. Rev. B **60**, 8783 (1999).
[39] A. Abragam, *Principles of Nuclear Magnetism* (Oxford University Press, Oxford, 1978).
[40] C. P. Slichter, *Principles of Magnetic Resonance* (Springer, Berlin, 1996).
[41] G. Schatz and A. Weidinger, *Nuclear Condensed Matter Physics* (Wiley, Chichester, 1996).
[42] K. D. Brommer, M. Galván, J. A. Dal Pino, and J. D. Joannopoulos, Surf. Sci. **314**, 57 (1994).
[43] C. Weindel, H. J. Jänsch, G. Kirchner, H. Kleine, J. J. Paggel, J. Roth, H. Winnefeld, and D. Fick, Phys. Rev. B **71**, 115318 (2005).
[44] H. J. Jänsch, G. Kirchner, O. Kühlert, M. Lisowski, J. J. Paggel, R. Platzer, R. Schillinger, H. Tilsner, C. Weindel, H. Winnefeld, and D. Fick, Nucl. Instrum. Methods Phys. Res. B **171**, 537 (2000).
[45] G. J. Pietsch, Appl. Phys. A: Mater. Sci. Process. **60**, 347 (1995).
[46] G. S. Higashi, R. S. Becker, Y. J. Chabal, and A. J. Becker, Appl. Phys. Lett. **58**, 1656 (1991).
[47] H. Winnefeld, Ph.D. thesis, Philipps-Universität (2000), electronic version: http://archiv.ub.uni-marburg.de/diss/z2001/0076.
[48] G. S. Higashi, Y. J. Chabal, G. W. Trucks, and K. Raghavachari, Appl. Phys. Lett. **56**, 656 (1990).
[49] H. D. Ebinger, H. Arnolds, C. Polenz, B. Polivka, W. Preyß, R. Veith, D. Fick, and H. J. Jänsch, Surf. Sci. **412/413**, 586 (1998).
[50] W. Preyß, H. D. Ebinger, H. J. Jänsch, R. Veith, D. Fick, M. Detje, C. Polenz, and B. Polivka, Hyperfine Interact. **110**, 295 (1997).
[51] C. Weindel, Ph.D. thesis, Philipps-Universität, Marburg, 2000.
[52] D. Fick, Hyperfine Interact. **136/137**, 467 (2001).
[53] J. Chrost and D. Fick, Surf. Sci. **343**, 157 (1995).
[54] H. Kleine, Ph.D. thesis, Philipps-Universität, Marburg, 1998.
[55] W. Mannstadt and G. Grawert, Phys. Rev. B **52**, 5343 (1995).
[56] M. Riehl-Chudoba, U. Memmert, and D. Fick, Surf. Sci. **245**, 180 (1991).
[57] N. Bloembergen, E. M. Purcell, and R. V. Pound, Phys. Rev. **73**, 679 (1948).
[58] W. W. Warren, Jr., Phys. Rev. B **3**, 3708 (1971).
[59] N. W. Ashcroft and N. D. Mermin, *Solid State Physics* (CBS, Asia, 1987).
[60] A. Zangwill, *Physics at Surfaces* (Cambridge University Press, Cambridge, 1988).
[61] R. Gomer, Rep. Prog. Phys. **53**, 917 (1990).
[62] H. Kleine and D. Fick, New J. Phys. **3**, 1.1 (2001).
[63] P. Pyykkö, Z. Naturforsch., A: Phys. Sci. **47a**, 189 (1992).
[64] T. Minamisono, T. Ohtsubo, I. Minami, S. Fukuda, A. Kitagawa, M. Fukuda, K. Matsuta, Y. Nojiri, S. Takeda, H. Sagawa, and H. Kitawgawa, Phys. Rev. Lett. **69**, 2058 (1992).
[65] H. J. Jänsch, M. Detje, H. D. Ebinger, W. Preyß, H. Reich, R. Veith, W. Widdra, D. Fick, M. Röckelein and H.-G. Völk, Nucl. Phys. A **568**, 544 (1994).
[66] C. Kittel, *Introduction to Solid State Physics*, 5th ed. (Wiley, New York, 1976).
[67] M. Kaack and D. Fick, Phys. Rev. B **51**, 17902 (1995).
[68] We call the energy distribution of the DOS and the model "schematic" to indicate that only its gross features are essential for the data analysis; the extremely narrow band at E_F embedded in a gap in between a broader occupied lower band and an empty upper one. All other features of the model, as e.g. the shape of the bands are assumed for convenience and are not checkable on the basis of the limited data set of Figs. 2 and 4.
[69] H. Ibach and H. Lüth, *Solid-State Physics* (Springer, Berlin, 2003).
[70] R. G. Chambers, *Electrons in Metals and Semiconductors* (Chapman and Hall, New York, 1990).
[71] A. Georges, G. Kotliar, W. Krauth, and M. J. Rozenberg, Rev.

Mod. Phys. **68**, 13 (1996).
[72] F. Flores, A. L. LevyYeyati, A. Martin-Rodero, and J. Merino, Phys. Low-Dimens. Semicond. Struct. **1**, 23 (1994).
[73] W. A. Harrison, Phys. Rev. B **31**, 2121 (1985).
[74] W. A. Harrison, *Elementary Electronic Structure* (World Scientific, Singapore, 1999).
[75] F. Bechstedt, A. A. Stekolnikov, J. Furthmüller, and P. Käckell, Phys. Rev. Lett. **87**, 016103 (2001).
[76] B. H. Bransden and C. J. Joachain, *Physics of Atoms and Molecules* (Longman, London, 1983).
[77] R. Neugart, Z. Phys. **261**, 237 (1973).
[78] W. Mönch, *Semiconductor Surfaces and Interfaces* (Springer-Verlag, Berlin, 1993).
[79] B. Horn, W. Dreves, and D. Fick, Z. Phys. B: Condens. Matter **48**, 335 (1982).